

NO-A190 440

REMOTE SENSING OF ATMOSPHERIC CROSSWINDS BY UTILIZING
SPECKLE-TURBULENCE (U) OREGON GRADUATE CENTER
BEAVERTON DEPT OF APPLIED PHYSICS AND E. J F HOLMES

1/1

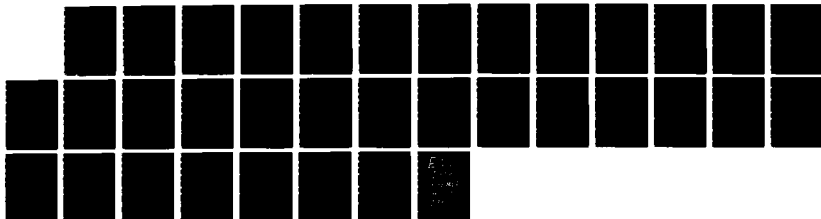
UNCLASSIFIED

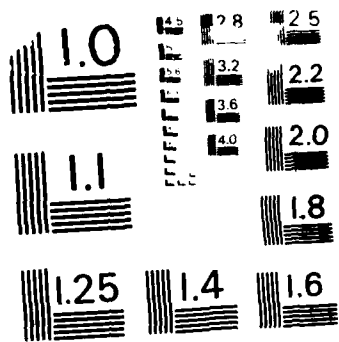
16 SEP 87 DAAL03-86-K-0022

F/G 4/2

ML

6





MICROCOPY RESOLUTION TEST CHART
NATIONAL BUREAU OF STANDARDS-1963-A

AD-A190 440

REPORT DOCUMENTATION PAGE

DTIC FILE COPY

Unclassified		1b. RESTRICTIVE MARKINGS	
2a. SECURITY CLASSIFICATION AUTHORITY		3. DISTRIBUTION/AVAILABILITY OF REPORT	
2b. DECLASSIFICATION/DOWNGRADING SCHEDULE		Approved for public release; distribution unlimited.	
4. PERFORMING ORGANIZATION REPORT NUMBER(S)		5. MONITORING ORGANIZATION REPORT NUMBER(S)	
6a. NAME OF PERFORMING ORGANIZATION Oregon Graduate Center	6b. OFFICE SYMBOL (if applicable) APEE	7a. NAME OF MONITORING ORGANIZATION U. S. Army Research Office	
6c. ADDRESS (City, State, and ZIP Code) 19600 N.W. Von Neumann Drive Beaverton, OR 97006-1999		7b. ADDRESS (City, State, and ZIP Code) P. O. Box 12211 Research Triangle Park, NC 27709-2211	
8a. NAME OF FUNDING/SPONSORING ORGANIZATION U. S. Army Research Office	8b. OFFICE SYMBOL (if applicable)	9. PROCUREMENT INSTRUMENT IDENTIFICATION NUMBER	
8c. ADDRESS (City, State, and ZIP Code) P. O. Box 12211 Research Triangle Park, NC 27709-2211		10. SOURCE OF FUNDING NUMBERS	
		PROGRAM ELEMENT NO.	PROJECT NO.
		TASK NO.	WORK UNIT ACCESSION NO.
11. TITLE (Include Security Classification) Remote Sensing of Atmospheric Crosswinds by Utilizing Speckle-Turbulence Interaction & Optical Heterodyne Detection			
12. PERSONAL AUTHOR(S) J. Fred Holmes			
13a. TYPE OF REPORT Final	13b. TIME COVERED FROM 1/1/86 TO 6/30/87	14. DATE OF REPORT (Year, Month, Day) 1987 September 16	15. PAGE COUNT 32
16. SUPPLEMENTARY NOTATION The view, opinions and/or findings contained in this report are those of the author(s) and should not be construed as an official Department of the Army position, policy, or decision, unless so designated by other documentation.			
17. COSATI CODES		18. SUBJECT TERMS (Continue on reverse if necessary and identify by block number)	
FIELD	GROUP	Remote Sensing, Atmospheric Winds, Laser, Speckle, Turbulence, Optical Heterodyne Detection	
19. ABSTRACT (Continue on reverse if necessary and identify by block number)			
Speckle-turbulence interaction can be utilized to measure the vector wind in a plane perpendicular to the line of sight from a laser transmitter to a target. A continuous wave source of around one watt and operating at 10.6 microns, in conjunction with an optical heterodyne receiver, has been used to measure atmospheric winds along horizontal paths. A theoretical basis, the experimental apparatus, processing techniques, and experimental results are presented. The technique has been demonstrated for remote sensing of atmospheric winds along horizontal paths and has potential for global remote sensing of atmospheric winds and for on-board wind shear detection systems for aircraft.			
20. DISTRIBUTION/AVAILABILITY OF ABSTRACT <input type="checkbox"/> UNCLASSIFIED/UNLIMITED <input type="checkbox"/> SAME AS RPT. <input type="checkbox"/> DTIC USERS		21. ABSTRACT SECURITY CLASSIFICATION Unclassified	
22a. NAME OF RESPONSIBLE INDIVIDUAL		22b. TELEPHONE (include Area Code)	22c. OFFICE SYMBOL E

Remote Sensing of Atmospheric Crosswinds by Utilizing
Speckle-Turbulence Interaction & Optical Heterodyne Detection

Final Report

by

J. Fred Holmes

16 September 1987

U.S. Army Research Office

Contract DAAL03-86-K-0022

Oregon Graduate Center
Department of Applied Physics and Electrical Engineering
19600 N.W. Von Neumann Drive
Beaverton, Oregon 97006-1999
(503) 690-1132

Approved for Public Release
Distribution Unlimited

88 1 27 047

Accession For	
NTIS GRA&I	<input checked="" type="checkbox"/>
DTIC TAB	<input type="checkbox"/>
Unannounced	<input type="checkbox"/>
Justification	
By _____	
Distribution/ _____	
Availability Codes	
Dist	Avail and/or Special
A-1	



THE VIEW, OPINIONS, AND/OR FINDINGS CONTAINED IN THIS REPORT ARE THOSE OF THE AUTHOR(S) AND SHOULD NOT BE CONSTRUED AS AN OFFICIAL DEPARTMENT OF THE ARMY POSITION, POLICY, OR DECISION, UNLESS SO DESIGNATED BY OTHER DOCUMENTATION.

Remote Sensing of Atmospheric Crosswinds by Utilizing Speckle-Turbulence Interaction & Optical Heterodyne Detection

Summary

Speckle-turbulence interaction can be utilized to measure the vector wind in a plane perpendicular to the line of sight from a laser transmitter to a target. A continuous wave source of around one watt and operating at 10.6 microns, in conjunction with an optical heterodyne receiver, has been used to measure atmospheric winds along horizontal paths. A theoretical basis, the experimental apparatus, processing techniques, and experimental results are presented. The technique has been demonstrated for remote sensing of atmospheric winds along horizontal paths; but also has potential for global remote sensing of atmospheric winds and for on-board wind shear detection systems for aircraft.

Research Progress

- o Designed, constructed and tested a 10.6 microns, cw, optical heterodyne transmitter receiver system for measuring atmospheric winds
- o Experimentally confirmed that speckle-turbulence interaction can be used to accurately measure atmospheric winds
- o Made measurements at target ranges of 500 m, 1000 m and 1300 m and at turbulence levels from $10^{-13} \text{ m}^{-2/3}$ to as low as $7.4 \times 10^{-16} \text{ m}^{-2/3}$ with good results
- o Discovered a novel method of isolating the optical local oscillator from the optical transmitter in optical heterodyne systems
- o Developed three new methods of processing the signals to obtain the wind

Additional detail is contained in the three progress reports for the subject contract, the publications and reports listed later in this final report, and in Appendix A which contains a preprint of a technical paper on this work.

Publications and Reports

J. Fred Holmes, Farzin Amzajerian, Rao V. S. Gudimetla, and John M. Hunt, "Remote Sensing of Atmospheric Winds by Utilizing Speckle-Turbulence Interaction, a CO₂ Laser and Optical Heterodyne Detection," submitted to Applied Optics.

John M. Hunt, J. Fred Holmes, and Farzin Amzajerian, "Optimum Local-Oscillator Levels for Coherent Detection Using Photoconductors," submitted to Applied Optics.

Douglas C. Draper, J. Fred Holmes, John M. Hunt, and John Peacock, "A simple system for frequency locking two CO₂ lasers," Proceedings of the Topical Meeting on Laser and Optical Remote Sensing, September 28 - October 1, 1987, Cape Cod, Massachusetts.

John M. Hunt, J. Fred Holmes, and Farzin Amzajerian, "Optimum local oscillator levels for coherent detection using photoconductors," Proceedings of the Topical Meeting on Laser and Optical Remote Sensing, September 28 - October 1, 1987, Cape Cod, Massachusetts.

J. Fred Holmes, Farzin Amzajerian, and John M. Hunt, "Improved optical local-oscillator isolation using multiple acousto-optic modulators and frequency diversity," Optics Letters 12, #8, page 637, August 1987.

V. S. Rao Gudimetla, J. Fred Holmes, "A two point joint density function of the intensity for a laser speckle pattern after propagation through the turbulent atmosphere," Proceedings of the Optical Society of America Annual Meeting, 19-24 October 1986, Seattle, Washington.

J. Fred Holmes, Farzin Amzajerian, V. S. Rao Gudimetla, John M. Hunt, "Remote Sensing of Atmospheric Winds Using a Coherent, CW Lidar and Speckle-Turbulence Interaction," Proceedings of the International Laser Radar Conference, August 11-15, 1986, Toronto, Canada.

J. Fred Holmes, John M. Hunt, Farzin Amzajerian, and V. S. Rao Gudimetla, "An Optical System for Remote Wind Sensing Using Speckle-Turbulence Interaction," Proceedings of the Conference on Lasers and Electrooptics, June 9-13, 1986, San Francisco, California.

(Invited) J. Fred Holmes, "Optical Remote Wind Measurement Using Speckle-Turbulence Interaction," Proceedings of the International Conference on Optical and Millimeter Wave Propagation and Scattering in the Atmosphere, May 27-30, 1986, Florence, Italy.

Three patents are in preparation on the system, the processing techniques and the local oscillator isolation technique.

SCIENTIFIC PERSONNEL SUPPORTED BY THIS PROJECT AND DEGREES AWARDED DURING THIS REPORTING PERIOD:

- Dr. J. Fred Holmes
- Dr. V. S. Rao Gudimetla
- Mr. John M. Hunt (Senior Engineer)
- Mr. Farzin Amzajerian (Ph.D. Student, Research Completed, Writing
Disseration)
- Mr. Douglas C. Draper (Ph.D. Student)
- Mr. John Peacock (M.S. Student)

Submitted to Applied Optics

**Remote Sensing of Atmospheric Winds by Utilizing
Speckle-Turbulence Interaction, a CO₂ Laser and Optical
Heterodyne Detection**

J. Fred Holmes, Farzin Amzajerdian, Rao V. S. Gudimetla, and John M. Hunt

Oregon Graduate Center

Department of Applied Physics and Electrical Engineering

19600 N.W. Von Neumann Drive

Beaverton, Oregon 97006-1999

ABSTRACT

Speckle-turbulence interaction can be utilized to measure the vector wind in a plane perpendicular to the line of sight from a laser transmitter to a target. A continuous wave source of around one watt and operating at 10.6 microns, in conjunction with an optical heterodyne receiver, has been used to measure atmospheric winds along horizontal paths. A theoretical basis, the experimental apparatus, processing techniques, and experimental results are presented. The technique has been demon-

strated for remote sensing of atmospheric winds along horizontal paths and has potential for global remote sensing of atmospheric winds and for on-board wind shear detection systems for aircraft.

Introduction

Speckle-turbulence interaction has the potential for allowing single ended remote sensing of the path averaged vector crosswind in a plane perpendicular to the line of sight to a target. If a laser transmitter is used to illuminate a target, the resultant speckle field generated by the target is randomly perturbed by the atmospheric turbulence as it propagates back to the location of the transmitter-receiver. When a crosswind is present, this scintillation pattern will move with time across the receiver aperture; and consequently, the time delayed statistics of the speckle field at the receiver are dependent on the crosswind velocity.

A continuous wave (cw) laser transmitter of modest power level in conjunction with optical heterodyne detection can be used to exploit the speckle-turbulence interaction and measure atmospheric winds. The use of a cw transmitter at 10.6 microns and optical heterodyne detection has many advantages including the availability of compact, reliable and inexpensive transmitters; better penetration of smoke, dust and fog; stable output power; low beam pointing jitter; and relatively simple receiver electronics. In addition, with a cw transmitter, options exist for processing the received signals for the crosswind that do not require a knowledge of the strength of turbulence.

It should be emphasized that the system to be described does not operate on the same principles as a doppler lidar remote wind sensing system [1]. The doppler systems use the aerosols in the atmosphere to scatter some of the transmitted energy from a coherent pulsed laser system back to a receiver where the doppler shift is used to measure the wind magnitude along the line of sight. The speckle-turbulence system uses a hard target as the scattering medium and measures the path averaged vector wind in a plane perpendicular to the line of sight. The two approaches compliment each other and each has certain advantages. A significant advantage of the doppler system is that

path resolved wind is easily obtained. There are potential methods such as crossed beams and multiple detectors for achieving some path resolution with a speckle-turbulence system; however, it would greatly complicate the system. The advantages of a speckle-turbulence system are the ability to measure the vector wind in a plane perpendicular to the line of sight and very simple equipment and data processing. By using optical heterodyne detection, only a watt or two of optical power is needed; and consequently, laser diodes could be used as the transmitter source. This should have a positive impact on portability and reliability.

An example of how well the speckle-turbulence system measures the wind is shown in Figure 1. The target was at 1 km and the turbulence level was intermediate at $2.37 \times 10^{-14} \text{ m}^{-2/3}$. Forty measurements with two and one-half second averages were made and the data was processed using a new method called the Binary-Z Log Ratio method that will be described later. There is some fluctuation about the mean due to the speckle; but the RMS error is only 0.33 m/s. The mean value of 2.01 meters/second averaged over the forty measurements compares well with the in situ measurement of 2.09 meters/second. Additional data will be shown in a later section including some data that demonstrates good operation at turbulence levels as low as $7.4 \times 10^{-16} \text{ m}^{-2/3}$.

Background

Analytic formulations for the first and second order statistics of the received intensity have been developed for the case where a diffuse target is illuminated by a TEM_{00} monochromatic laser beam [2,3]. They properly account for the effect of atmospheric turbulence both for propagation of the laser beam from the transmitter to the target and propagation of the target induced speckle field back to the receiver. The exact formulations are quite complex and difficult to interpret. However, for longer wavelength

sources such as 10.6 microns, simple formulations based on the joint Gaussian assumption are valid for turbulence levels corresponding to Rytov variances less than about 0.02 and are much easier to deal with initially.

From previous work, the time lagged covariance (TLC) function of the intensity using the joint Gaussian assumption is given for the focused case by [2]

$$C_I(\mathbf{P}, \mathbf{V}\tau) = \langle (I(\mathbf{P}_2, t_2) - \langle I \rangle) (I(\mathbf{P}_1, t_1) - \langle I \rangle) \rangle$$

$$= \langle I \rangle^2 \exp \left[\frac{-P^2}{2\alpha_0^2} - 5.82 Lk^2 \int_0^1 C_n^2(w) |(1-w)\mathbf{P} - \mathbf{V}\tau|^{5/3} dw \right] \quad (1)$$

where \mathbf{P}_i designates the location of a detector in the receiver plane,

$$\mathbf{P} = \mathbf{P}_2 - \mathbf{P}_1$$

$$\tau = t_2 - t_1$$

α_0 = Transmitter Beam Radius

C_n^2 = Strength of Turbulence

L = Path Length

\mathbf{V} = Vector Wind Velocity

k = Wave Number

and

w = Normalized Path Length from the Transmitter-Receiver to the Target

As can be seen from Eq.(1), if two detectors are separated by a vector distance \mathbf{P} , the TLC can be measured; and the measured quantity will be a function of the vector wind velocity. In the next section it will be seen how to exploit this relationship and measure atmospheric winds.

Processing Techniques

There are several well known processing techniques that should be useful in determining the wind from the received signal. Some of these techniques are illustrated in Figure 2. The Briggs method measures the time delay, τ_B , at which the autocovariance and TLC curves cross. The delay to peak method measures the time delay, τ_p , where the TLC curve peaks. The width of the autocovariance method measures the time delay, τ_w , at which the autocovariance curve decreases to 67% of its peak value. The slope method measures the slope of the TLC at zero time delay. In order to process the signals for the wind, the relationships between the time delays, slope, and the wind must be derived using Eq.(1). It will be found that the delay to peak and Briggs techniques yield the wind directly; whereas the width of the autocovariance and slope techniques either require a knowledge of ρ_o , the transverse phase coherence length, or must be used in conjunction with one of the other techniques to determine the wind and ρ_o .

The time delay to the peak of the TLC function can be found from Eq.(1) by differentiating with respect to τ and setting the resulting equation to zero. Before proceeding, Eq.(1) will be examined in a slightly different form that eliminates the absolute value and assumes uniform wind and turbulence. The desired form is

$$C_1(\vec{P}, \vec{V}\tau) = \langle I \rangle^2 \exp \left[\frac{-P^2}{2\alpha_o^2} - \frac{32}{3} \left(\frac{V}{\rho_o} \right)^{5/3} \int_0^1 \left[(1-w)^2 P^2 - 2(1-w) P V \tau \cos\theta + (V\tau)^2 \right]^{5/6} dw \right] \quad (2)$$

where θ is the angle between \vec{P} and \vec{V} . Differentiating Eq.(2) with respect to τ and setting the result equal to zero yields

$$\int_0^1 \left[(1-w)^2 - 2(1-w) x \cos\theta + x^2 \right]^{-1/6} \left[(1-w) \cos\theta - x \right] dw = 0 \quad (3)$$

where

$$x = \frac{V\tau_p}{P} \quad (4)$$

For the case where \mathbf{V} and \mathbf{P} are horizontal and V is uniform along the path, Eq.(3) can be solved analytically with the result that $x = 1/2$ or

$$V = \frac{P}{2\tau_p} \quad (5)$$

For the case where \mathbf{P} is orthogonal to \mathbf{V} , the solution to Eq.(3) is $x = 0$ with the result that there is no shift of the peak of the time delayed covariance function from zero and consequently no sensitivity to that component of the wind. The relative wind sensitivity function for the time delay to peak method can be found using Eq.(1) and reformulating Eq.(3). Numerical work indicated that the relative sensitivity function on x is

$$x(w) = (1-w)\cos\theta \quad (6)$$

Consequently the relative weighting on τ_p the measured quantity is $(1-w)$, so it would appear that the relative weighting on the measured wind along \mathbf{P} is $1/(1-w)$. It should be noted that the relative wind sensitivity function is not the conventional wind weighting function. Because Eq.(3) is a non-linear function of the wind, a linear wind weighting function cannot be defined. However, the relative wind sensitivity function does give the relative contribution to the result of each part on the path for equal values of wind.

The slope of the TLC function can also be used to process the data. Using Eq.(1) the slope is given by

$$S_I = \left. \frac{\partial}{\partial \tau} C_I(\bar{P}, \nabla \tau) \right|_{\tau=0}$$

$$= C_I(\bar{P}, 0) \left(\frac{32}{3} \right) (5/3) (0.546 Lk^2) P^{2/3} \int_0^1 dw C_n^2(w) V_p(w) (1-w)^{2/3} \quad (7)$$

where V_p is the component of wind along \bar{P} . From Eq.(7) it can be seen directly that the wind weighting function is $(1-w)^{2/3}$ and that the slope method of processing is sensitive only to the wind along \bar{P} . Consequently, with two orthogonal sets of detectors, the vector wind in the plane perpendicular to the line of sight can be found. When the wind and turbulence are uniform, Eq.(7) reduces to

$$S_I = C_I(P, 0) \frac{32}{3} \frac{P^{2/3}}{\rho_0^{5/3}} V_p \quad (8)$$

which can be used to find V_p from measurements of the slope and covariance, $C_I(P, 0)$. Unfortunately Eq.(8) also depends on ρ_0 which is not known. Consequently, the slope method of processing must be used in conjunction with one of the other methods in order to be useful.

The Briggs method measures the time delay at which the autocovariance and time delayed covariance curves cross. For speckle-turbulence interaction, a slightly modified definition as illustrated in Eq.(9) is used.

$$\exp[P^2/2\alpha_0^2] C_I(\bar{P}, \tau) = C_I(0, \tau) \quad (9)$$

Using Eq.(2) in Eq.(9), the expression becomes

$$\int_0^1 [(1-w^2)y^2 - 2(1-w) y \cos\theta + 1]^{5/6} dw \quad (10)$$

where

$$y = \frac{P}{V_{\tau B}} \quad (11)$$

Numerical work indicates that using

$$y = 3.1056 \cos\theta \quad (12)$$

yields values of y accurate to within 0.05. Consequently, the wind when it is aligned with \mathbf{P} is given by

$$V = \frac{P}{3.1056 \tau_B} \quad (13)$$

For the vector wind case, three or more detectors are used to form an array where there are two vector spacings \mathbf{P}_1 and \mathbf{P}_2 that are orthogonal (another possibility is three detectors in an equilateral triangle). In this case

$$y_1 = \frac{P_1}{V\tau_{B1}} = 3.1056 \cos\theta_1 \quad (14)$$

$$y_2 = \frac{P_2}{V\tau_{B2}} = 3.1056 \cos\theta_2 = 3.1056 \sin\theta_1 \quad (15)$$

$$\text{where } \theta_2 = \theta_1 - 90^\circ \quad (16)$$

Taking the ratio of Eqs.(14) and (15) yields

$$\frac{y_1}{y_2} = \frac{P_1\tau_{B2}}{P_2\tau_{B1}} = \cot\theta_1 \quad (17)$$

From the time delay measurements and the known detector spacings, the angle θ_1 can be determined. The two wind components are then given by

$$V_1 = \frac{\mathbf{V} \cdot \mathbf{P}_1}{P_1} = V \cos\theta_1 = \frac{P_1}{3.1056 \tau_{B1}} \quad (18)$$

$$V_2 = \frac{\mathbf{V} \cdot \mathbf{P}_2}{P_2} = V \sin\theta_1 = \frac{P_2}{3.1056 \tau_{B2}} \quad (19)$$

The relative wind sensitivity function for the Briggs method was not determined. However, numerical work using a 60% sinusoidally modulated wind showed very little difference from the case where the wind was constant.

Another method that may be useful in processing the data is the autocovariance width. In this method, the time delay at which the autocovariance falls to a prescribed value is used. For speckle-turbulence interaction, the slope of the autocovariance curve is a maximum when

$$C_I(0, V\tau_w) = e^{-0.4} \quad (20)$$

which yields

$$V/\rho_0 = \frac{0.139}{\tau_w} \quad (21)$$

As can be seen from Eq.(21), the strength of turbulence must be known in order to find the wind using the width of the autocovariance processing method. However, it can be used with other methods such as the slope method to find both V and ρ_0 . In addition, it should be noted that this method has no sensitivity to the direction of the wind. The relative sensitivity of the width of the autocovariance method to wind at different points along the path has been determined numerically to be uniform. It is however, non-linear with respect to the magnitude of the wind.

All of the above methods have been used to process data collected by the experimental apparatus. However, the results obtained were not very good. It is believed that the reason for this is the rather small effect that the turbulence has on the time delayed covariance function at 10.6 microns wavelength. As an example, for a 1000 meter path-length, 10.6 microns wavelength and $C_n^2 = 10^{-13} \text{ m}^{-2/3}$, the peak of the TDC rises only 2.5% above the value at zero time delay. These small changes coupled with having to find them in a fully developed speckle pattern makes processing difficult. However, it should be noted that the above techniques should be usable at much shorter wavelengths where the speckle-turbulence interaction is stronger and past work in the near infrared [4] tends to confirm that conclusion.

Because of these difficulties with the above techniques an effort, which turned out to be quite successful, was made to develop a new processing technique. This technique will be referred to as the Z Log Ratio (ZLR) method. Two parameters B and C are defined as

$$B = \frac{C_I(0,\tau)}{\sigma_I^2} = \exp \left[- \frac{32}{3} \left(\frac{P}{\rho_o} \right)^{5/3} |x|^{5/3} \right] \quad (22)$$

$$C = \frac{C_I(P,o)}{\sigma_I^2} = \exp \left[- \frac{P^2}{2\alpha_o^2} - \frac{32}{3} \left(\frac{P}{\rho_o} \right)^{5/3} \frac{3}{8} \right] \quad (23)$$

$$X = \frac{V\tau}{P} \quad (24)$$

where use was made of Eq.(2). Now using Eqs.(22) and (23) the ZLR is defined as

$$Z = \frac{\ln B}{\ln C + P^2/2\alpha_o^2} = \frac{8}{3} |X|^{5/3} \quad (25)$$

from which the wind velocity can be derived as

$$V = \left(\frac{3}{8} \right)^{3/5} \frac{Z^{3/5} P}{|\tau|} \quad (26)$$

As will be seen in a later section, good results have been achieved using the ZLR method. The quantities B and C are derived from the received signals, used in Eq.(25) to calculate Z which is used in (26) to obtain the magnitude of the wind. It should be noted that there are no arbitrary parameters used in the formulation; and the only system parameters needed are the spacing between the detectors and the transmitted beam radius. Since Eq.(26) does not yield the direction of the wind, for the case where the wind is aligned along \bar{P} , the sign of the measured slope of the TLC can be used for that purpose. Numerical analysis indicates that the wind sensitivity function for the ZLR processing technique is uniform.

The ZLR method may also be used for the vector wind case. Since Eq.(26) depends on the magnitude of the vector wind, it is still valid. All that remains is to find the angle between \bar{P} , and the vector wind. If the slope is measured using two sets of orthogonal detectors with spacings P_1 and P_2 , then the ratio of the slopes yields

$$\frac{S_1}{S_2} = \frac{C_1(P_1,0)}{C_1(P_2,0)} \left(\frac{P_1}{P_2} \right)^{2/3} \cotan\theta_1 \quad (27)$$

which reduces to

$$\frac{S_1}{S_2} = \cotan\theta_1 \quad (28)$$

for $P_1 = P_2$. The two components of the wind then are given by

$$V_1 = V \cos\theta_1 \quad (29)$$

and

$$V_2 = V \sin\theta_1 \quad (30)$$

In practice, Z is measured at several time delays and the results averaged. If this is done then

$$|V| = \left(\frac{3}{8} \right)^{3/5} \frac{P}{N} \sum_{n=1}^N \frac{Z_n^{3/5}}{\tau_n} \quad (31)$$

where Z_n is the measured value of Z at time delay τ_n . Most of the wind data shown in the next section was processed using Eq.(31).

In an attempt to further improve the ZLR method, it has been reformulated into a result that minimizes the mean square error on the measured quantity Z_n . The mean square error is given by

$$MSE = \frac{1}{N} \sum_{n=1}^N \left[Z_n - \frac{8}{3} \left(\frac{V^2 \tau_n^2}{P^2} \right)^{5/6} \right]^2 \quad (32)$$

Using

$$\frac{\partial \text{MSE}}{\partial V} = 0 \quad (33)$$

the wind velocity that minimizes the mean square error is given by

$$V_{\text{MMSE}} = P \left[\frac{3/8 \sum_{n=1}^N Z_n |\tau_n|^{5/3}}{\sum_{n=1}^N |\tau_n|^{10/3}} \right]^{3/5} \quad (34)$$

Now putting Eq.(34) back into Eq.(32) the minimum mean square error is found as

$$\text{MMSE} = \frac{1}{N} \left[\sum_{n=1}^N Z_n^2 - \left(\sum_{n=1}^N Z_n |\tau_n|^{5/3} \right)^2 / \sum_{n=1}^N |\tau_n|^{10/3} \right] \quad (35)$$

The use of Eq.(34) usually produces slightly better results than Eq.(31). It is proposed that Eq.(35) might be used as a "goodness" measure on the data.

In a subsequent section the experimental results using Eq.(31) and Eq.(34) will be presented along with one more variation on the processing that gives both a better estimate of the wind and significantly reduces the statistical fluctuation in the measurement. The data is preprocessed to yield a one bit per sample binary data set. This is accomplished by letting the bit be one or zero depending on whether the received intensity is greater than or less than the mean respectively. This also significantly decreases the processing time required and will make designing a portable instrument much easier. This technique will be referred to as Binary-Z Log Ratio (B-ZLR) processing.

Experimental Design

The transmitter/receiver optical design is shown in Figure 3. The source is a CO_2 waveguide laser operating at 10.6 microns wavelength. The laser beam is first expanded by a factor of 3 and then most of the beam is split off by a 90° beam splitter and

directed through an acoustooptic modulator (AOM) used as a frequency shifter and driven at 37.5 MHz. The frequency shifted beam at a little over one watt of power then passes through a quarter-wave plate to produce a circularly polarized beam that is focused onto the target by a 10 X beam expander. The half-wave plate at the output of the 3 X beam expander is used to change the polarization of the laser beam from vertical to horizontal to match the requirements of the AOM. A circularly polarized beam is transmitted in order to eliminate fluctuations in the returned signal due to target induced polarization changes.

Approximately 10% of the laser beam passes through the 90% beam splitter for use as an optical local oscillator. It passes through a second AOM which is also used as a frequency shifter and driven at 42.5 MHz. The purpose of the second AOM is to provide isolation between the transmitted beam and the local oscillator. An isolation of over 200 db has been achieved [5] which is sufficient not to degrade the extreme sensitivity of optical heterodyne detection. The frequency shifted local oscillator beam is then circularly polarized by a quarter-wave plate to match the transmitted beam, split into two parts and focused onto two HgCdTe detectors. The detectors are photovoltaic, 0.2 mm square and were housed in separate dewars to allow some flexibility in selecting the spacing between the detectors and to simplify the optical design.

The transmitted beam is scattered diffusely by a 4 foot \times 4 foot sandblasted aluminum target. The speckle field that is generated by the target and modulated by the turbulence in the atmosphere returns to the transmitter/receiver where it is directed by two, one-inch mirrors set at 45 degrees onto lenses that focus it onto the detectors. The returned signal and the optical local oscillator photomix at the detector to produce a heterodyne signal at their difference frequency of 5 MHz. This signal is then processed to obtain the wind. Since the detectors are spaced horizontally, the system measures

the horizontal component of the wind. If the vector wind were to be measured, then a minimum of one more detector, spaced vertically, would be required.

The receiver electronics for one channel is illustrated in Figure 4. The heterodyne signal current at 5 MHz from each detector is amplified, filtered, mixed down to 100 kHz, precision rectified to recover the field amplitudes, and low pass filtered before being digitized for processing. Because the interaction with the turbulence is small, good linearity (0.1%) and stability are required. The received intensities are recovered by squaring the measured amplitudes in a computer.

Experimental Results

Measurements were made using 500 meter and 1000 meter paths over very flat, featureless terrain where the turbulence is quite uniform over the path. In situ data was taken using a Campbell Scientific CA-9 path averaging scintillometer and crosswind sensor. The Campbell unit is a double ended unit with a transmitter at one end and a receiver at the other and has a cosine-like wind sensitivity function; whereas the heterodyne system, utilizing the ZLR method of processing has a uniform wind sensitivity function. Since the wind was not uniform along the path, some of the differences between the heterodyne measurements and the in situ data may be attributed to the difference in their wind sensitivity functions. Figures 5 and 6 show wind magnitude data taken with the target at 500 and 1000 meters, with approximately 2 and 4 meters per second wind respectively and at an intermediate level of turbulence. The overall results are good. There is moderate statistical fluctuation about the mean due to the speckle and short averaging times; but the mean values averaged over the 100 seconds of data are within 0.12 and 0.54 m/sec respectively of the in situ measurements. It should be noted that the fluctuation can be reduced either by longer time averages

and/or by using additional detectors and spatial averaging. In addition, as will be demonstrated later in this section, the use of B-ZLR or MMSE processing also reduces the fluctuation due to speckle. The wind direction was determined by the sign of the slope. For the second averages, the correct sign of the slope was measured about 70% of the time. This result is not as good as was expected; and work is continuing to improve the processing.

An important consideration in using speckle-turbulence interaction for measuring winds is operation at low turbulence levels. An estimate of the lower limit at which this type of system should operate will be made, followed by some experimental work at low turbulence.

An estimate of the sensitivity of the experimental system can be made by considering Eq.(8). Since the slope is proportional to C_n^2 , as C_n^2 decreases the slope decreases and eventually a limit will be reached below which the system will not respond. Also there are deterministic (as opposed to random) errors such as gain drifts for the two optical channels that do not average to zero. Consequently, it is doubtful that the system can measure the received intensity normalized by the mean to better than one-tenth of one percent. This translates to no worse than four-tenths of one percent on the normalized slope. Using this with Eq.(8), it is found that

$$C_n^2 \geq \frac{1.741 \times 10^{-5} \lambda^2}{L P^{2/3} V_p C_I(P)} \quad (36)$$

It can be seen that as the wavelength λ decreases and the path length increases, the sensitivity improves. For the experimental system under consideration and with $L = 1000$ m and $V_p = 1$ m/s, Eq.(36) becomes

$$C_n^2 \geq 3 \times 10^{-17} \text{ m}^{-2/3} \quad (37)$$

This is the minimum C_n^2 at which the system is expected to respond under the conditions given and appears to be low enough to make the proposed technique quite useful. It is expected then, that a system of this type should provide good measurements at C_n^2 levels around 10 times the level predicted by (37) or $3 \times 10^{-16} \text{ m}^{-2/3}$.

Figure 7 shows a data set processed using the ZLR method and corresponding to $C_n^2 = 7.4 \times 10^{-16} \text{ m}^{-2/3}$ which constitutes a low value of turbulence. There is the usual fluctuation about the mean and the mean value of 1.64 m/sec averaged over the 100 seconds of the data set, is less than the mean value of 1.96 m/sec measured by the Campbell unit. This reduction in mean value is believed to be indicative that the system is just beginning to lose sensitivity (with ZLR processing).

Figure 8 shows this same data set processed using the MMSE method and it can be seen that the error in the mean is comparable to the ZLR method; but the statistical fluctuations are reduced yielding an rms error of 0.56 m/sec as opposed to 0.79 for ZLR processing.

The results of processing this data using the B-ZLR method are shown in Figure 9. There is a substantial reduction in error and fluctuation as compared to the results obtained by ZLR processing. The mean error was only 0.15 m/sec and the RMS error only 0.35 m/sec. Processing the data using the binary data set and the MMSE method did not yield results any better than the B-ZLR method. Considering that the MMSE method requires more processing than the ZLR method it is concluded that the best of the methods that were considered is the B-ZLR method of processing and that good measurements can be made at turbulence levels down into the $10^{-16} \text{ m}^{-2/3}$ range.

Acknowledgement

This work was supported by the U.S. Army Research Office.

References

- [1] Robert T. Menzies, "Doppler Lidar Atmospheric Wind Sensors: A Comparative Performance Evaluation for Global Measurement Applications from Earth Orbit," *Applied Optics*, **25**, 1 August 1986.
- [2] Myung Hun Lee, J. Fred Holmes, and J. Richard Kerr, "Statistics of speckle propagation through the turbulent atmosphere," *J. Opt. Soc. Am.* **66**, November 1976.
- [3] J. Fred Holmes, Myung Hun Lee, and J. Richard Kerr, "Effect of the log-amplitude covariance function on the statistics of speckle propagation through the turbulent atmosphere," *J. Opt. Soc. Am.* **70**, April 1980.
- [4] J. Fred Holmes, "Optical Remote Wind Measurement Using Speckle-Turbulence Interaction," *Proceedings of the Optical Society of America Conference on Optical and Millimeter Wave Propagation and Scattering, Florence, Italy, May 27-30, 1986.*
- [5] J. Fred Holmes, Farzin Amzajerdian, and John M. Hunt, "Improved Optical Local Oscillator Isolation Using Multiple Acousto-optic Modulators and Frequency Diversity," *Optics Letters*, **12**, August 1987.

List of Figures

Figure 1 - Wind Measurement, Target at 1.0 Km, Binary-Z Log Ratio Processed

Figure 2 - Processing Techniques

Figure 3 - Transmitter/Receiver Optical Design

Figure 4 - Receiver Electronics

Figure 5 - Wind Measurement, Target at 500 Meters, Z Log Ratio Processed

Figure 6 - Wind Measurement, Target at 1000 Meters, Z Log Ratio Processed

Figure 7 - Low Turbulence Wind Measurement, Z Log Ratio Processed

Figure 8 - Low Turbulence Wind Measurement, Minimum Mean Square Error Processed

Figure 9 - Low Turbulence Wind Measurement, Binary-Z Log Ratio Processed

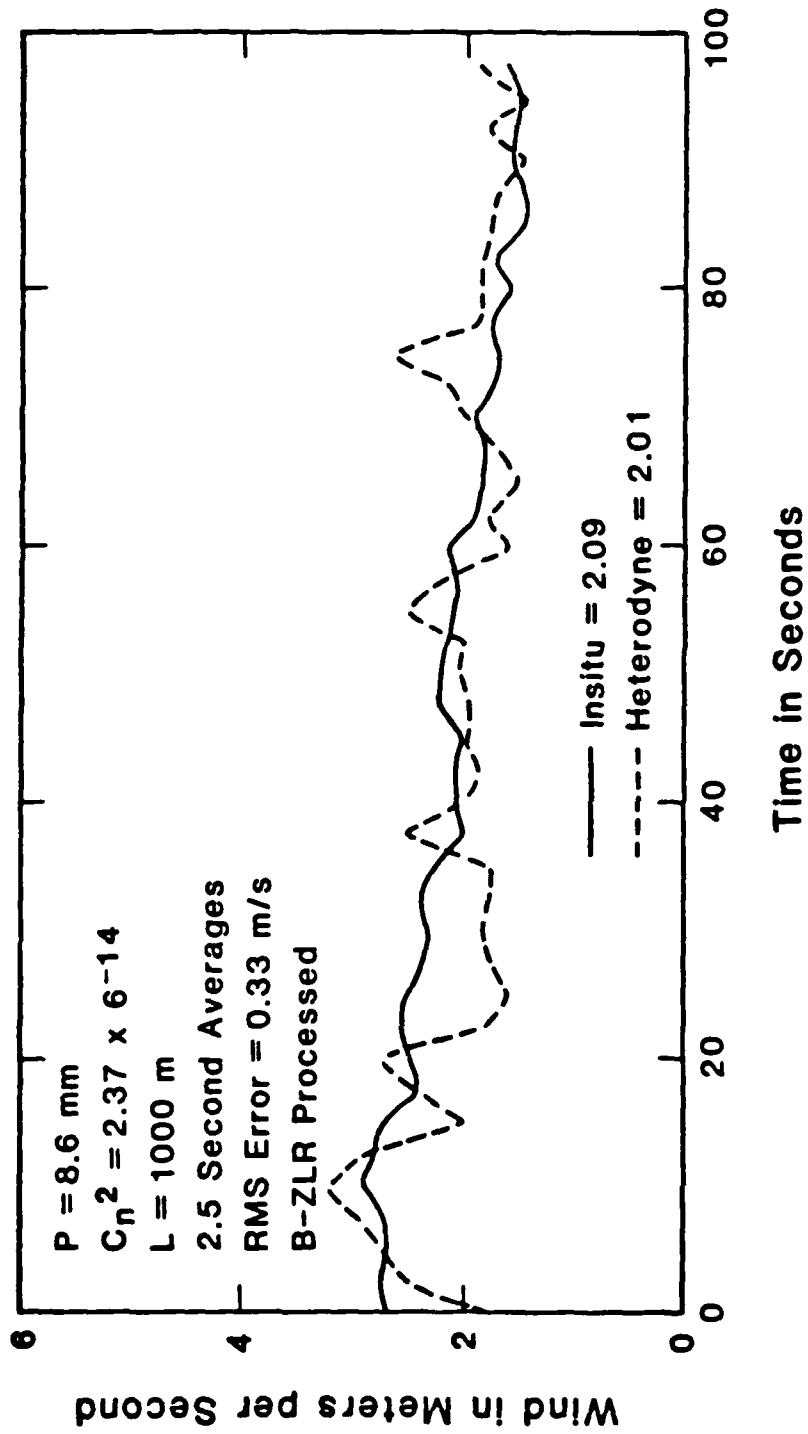


Figure 1 - Wind Measurement, Target at 1.0 Km, Binary-Z Log Ratio Processed

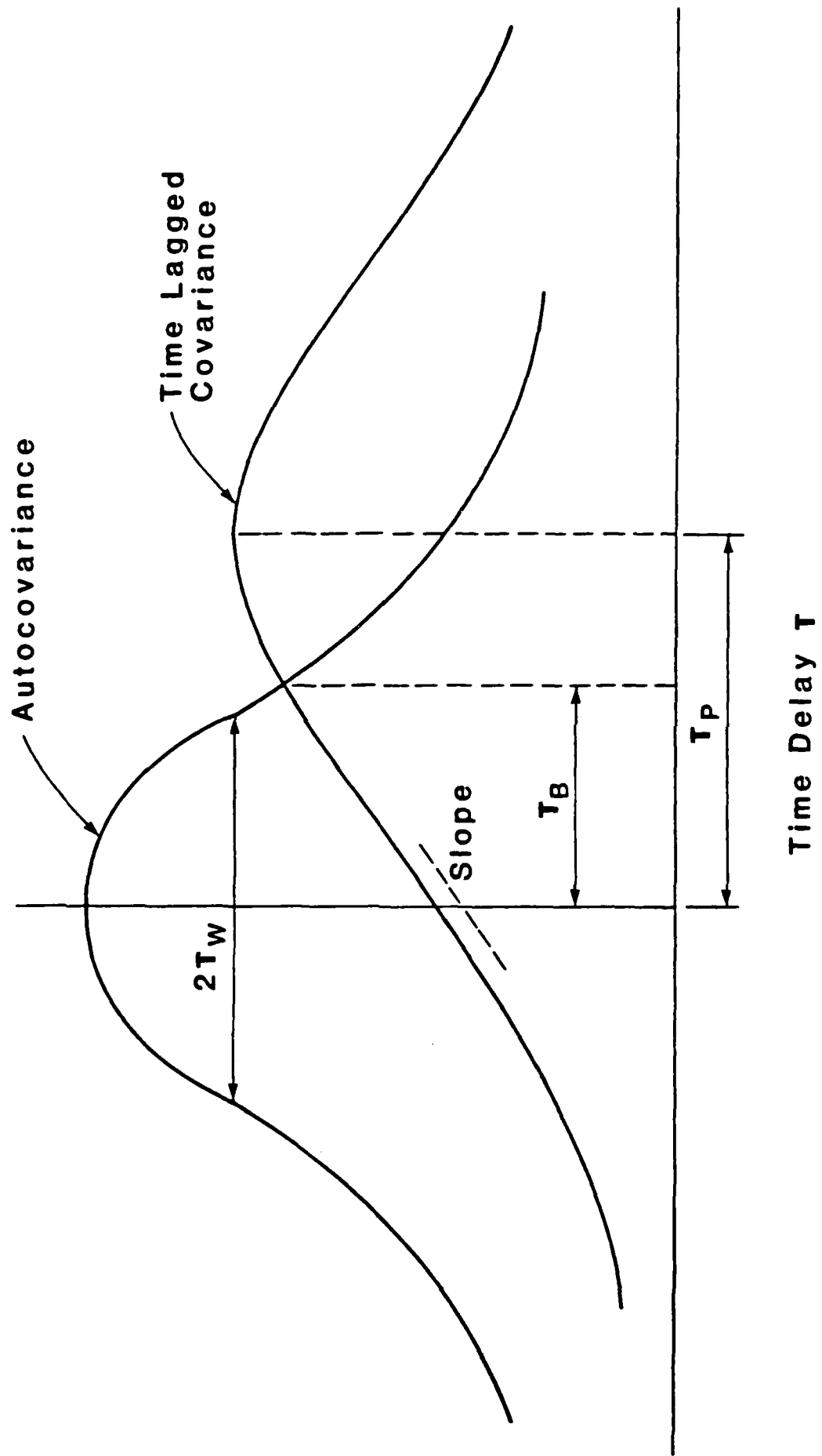


Figure 2 - Processing Techniques

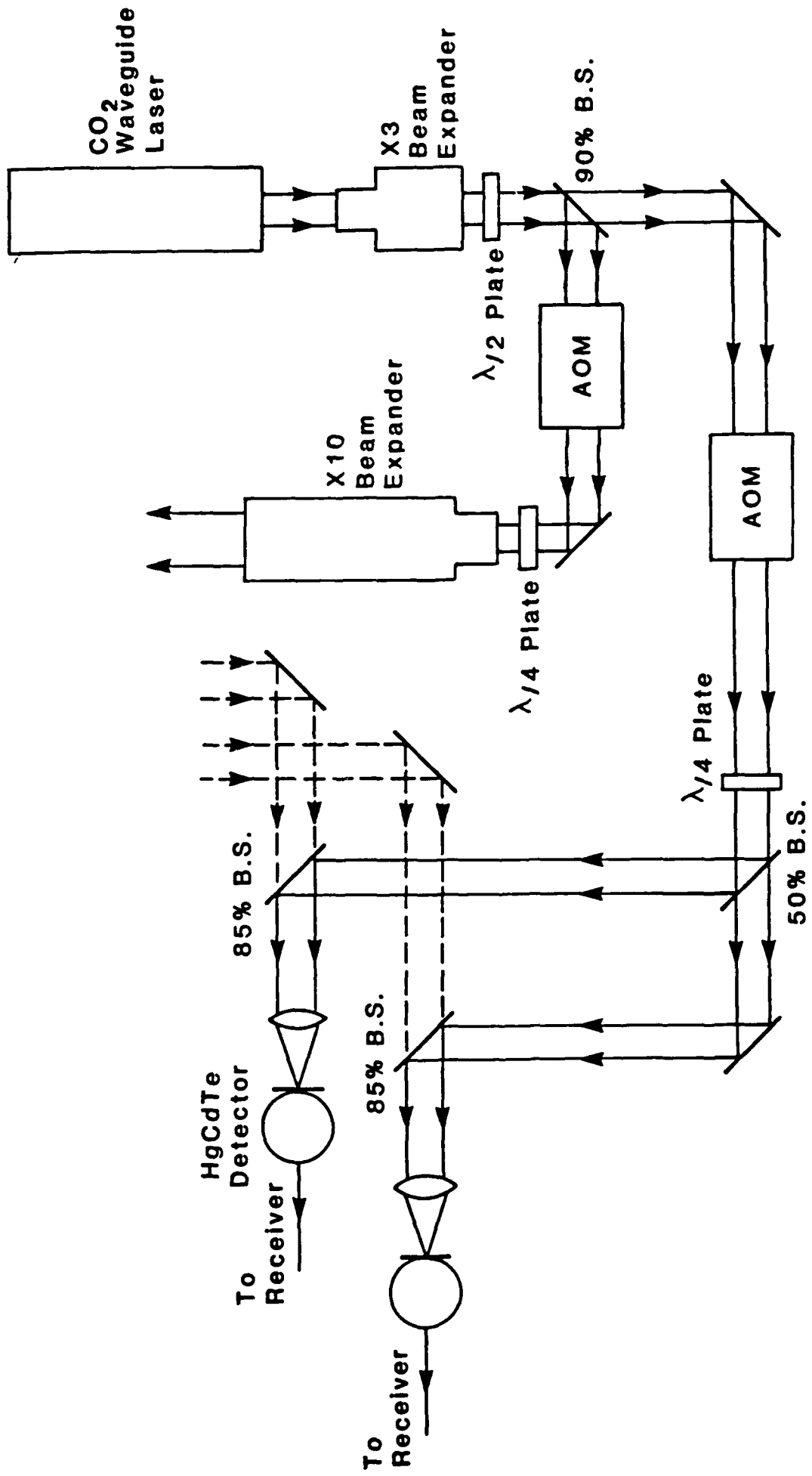


Figure 3 - Transmitter/Receiver Optical Design

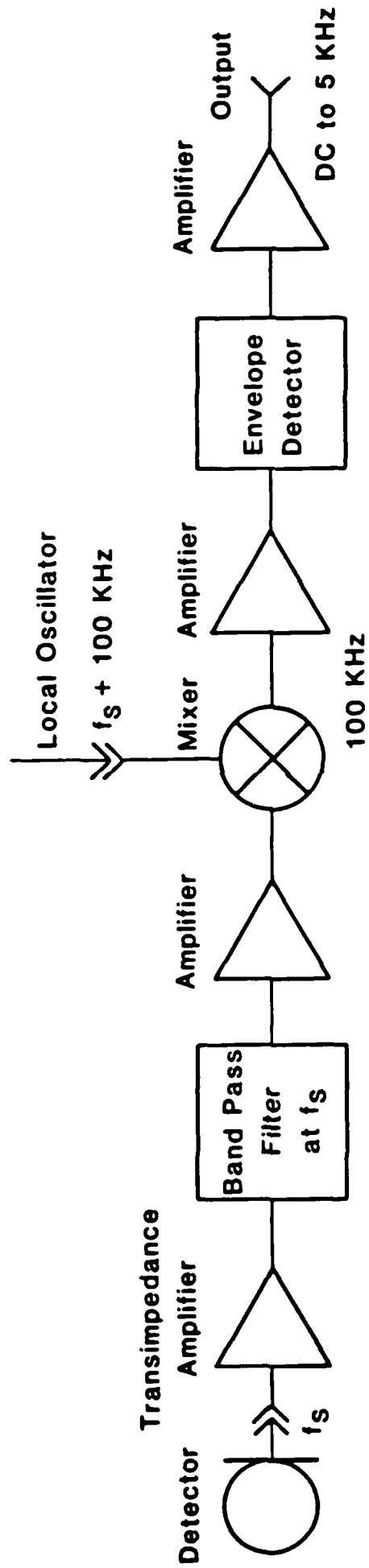


Figure 4 - Receiver Electronics

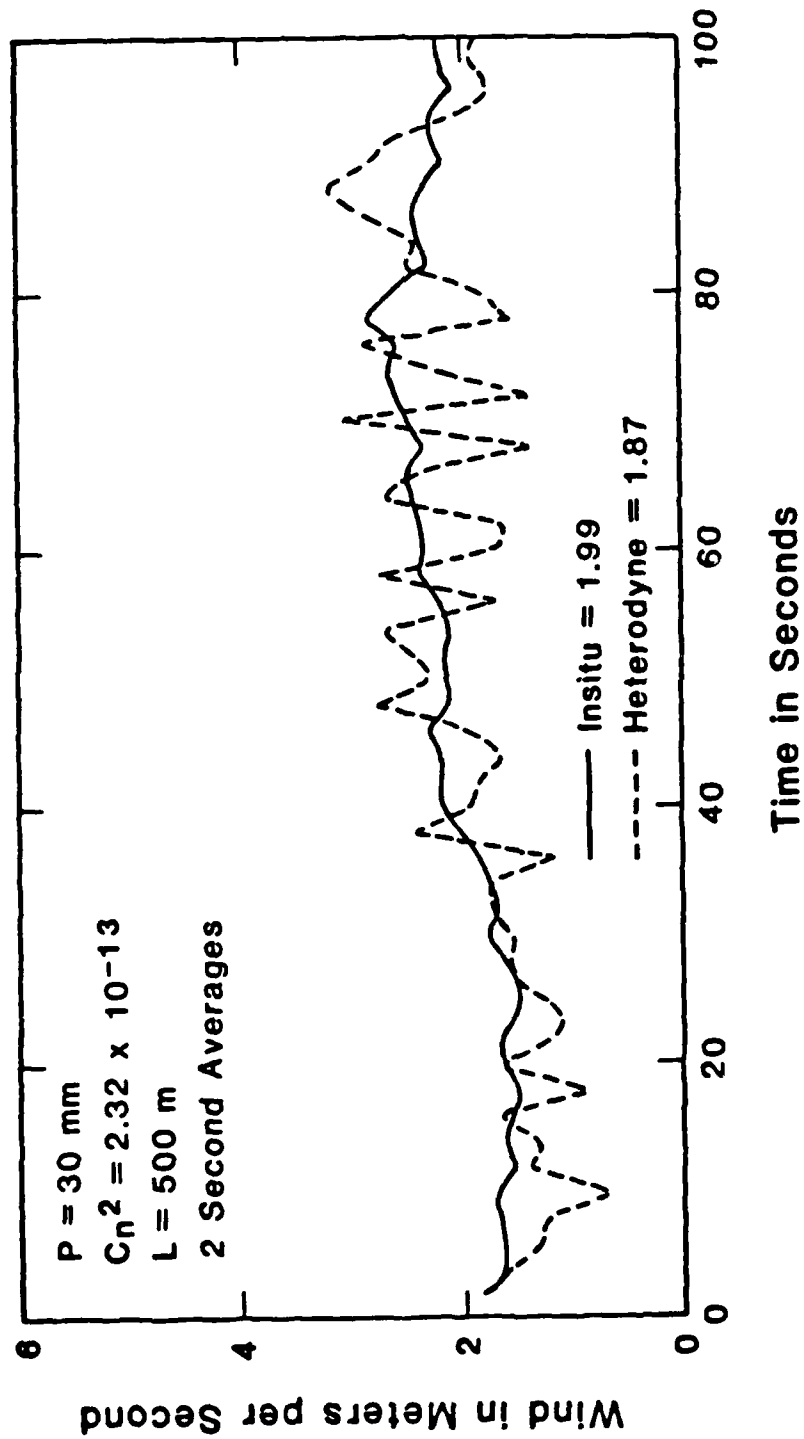


Figure 5 - Wind Measurement, Target at 500 Meters, Z Log Ratio Processed

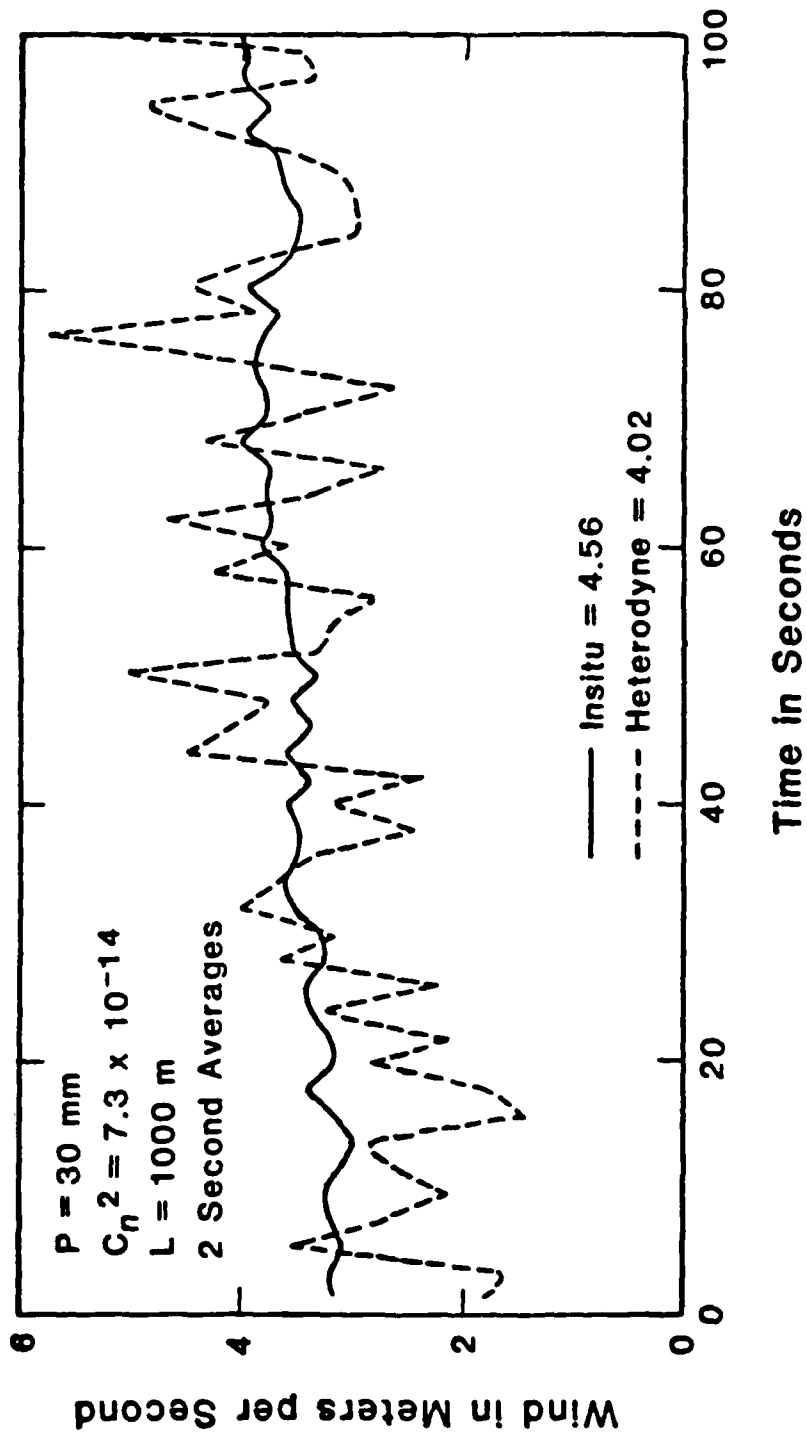


Figure 6 - Wind Measurement, Target at 1000 Meters, Z Log Ratio Processed

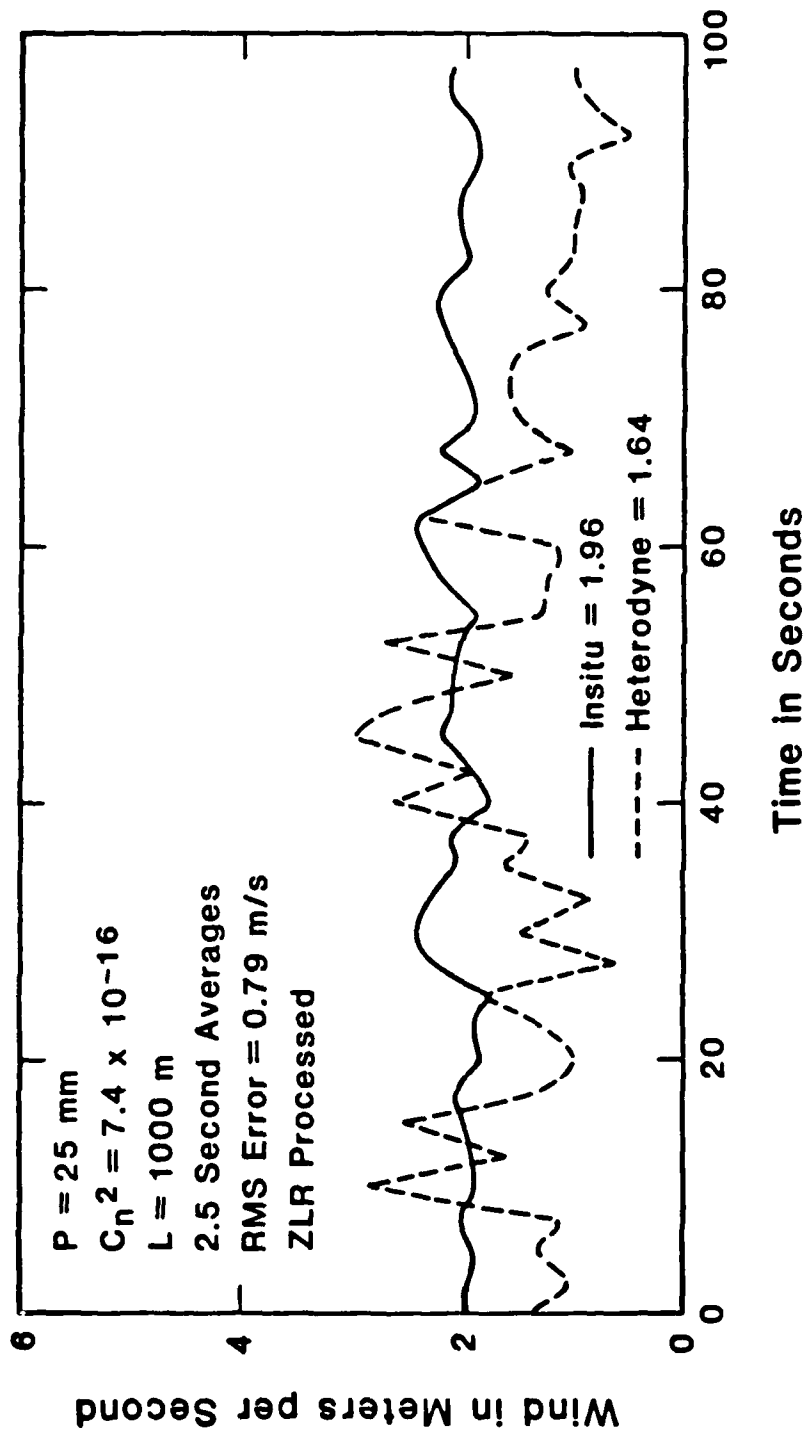


Figure 7 - Low Turbulence Wind Measurement, Z Log Ratio Processed

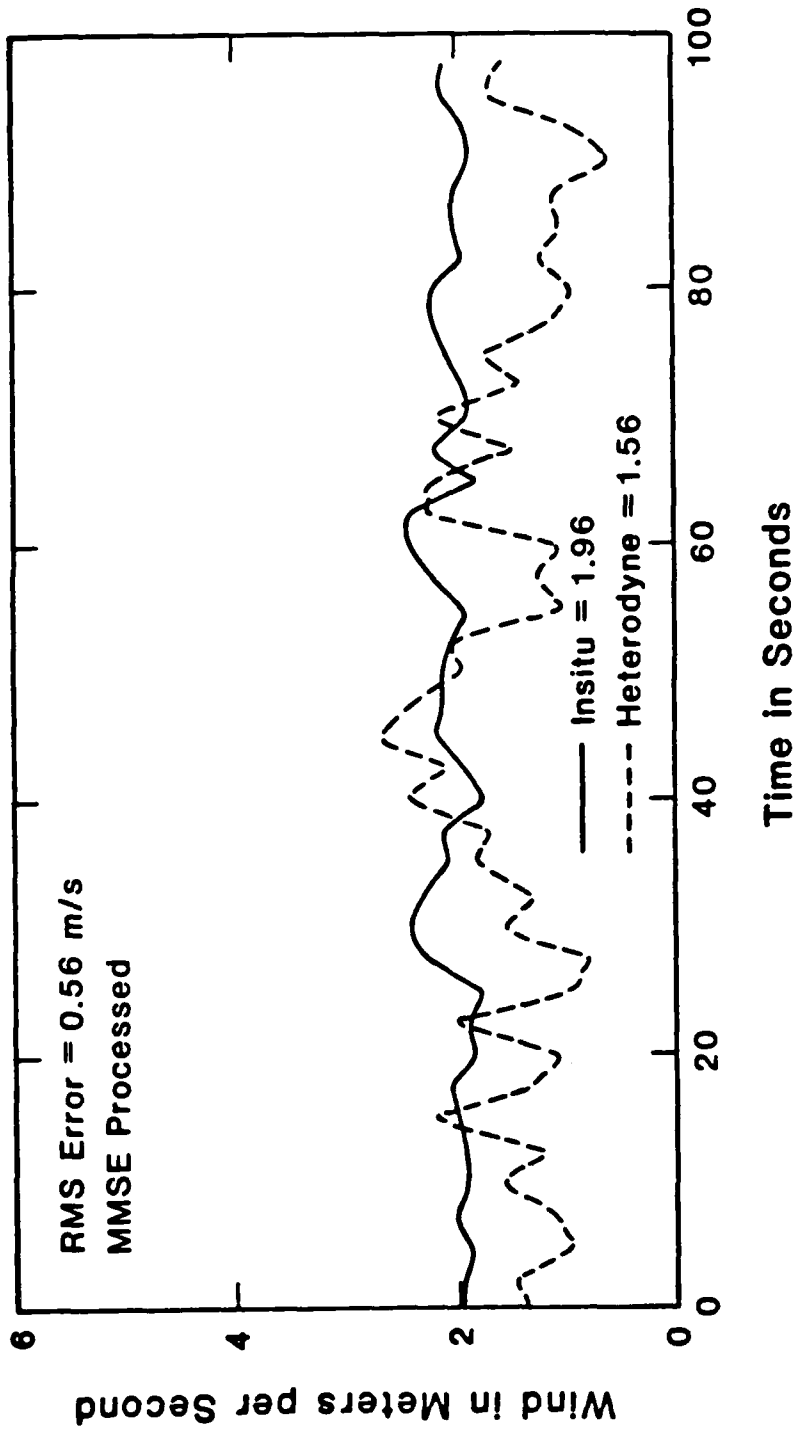


Figure 8 - Low Turbulence Wind Measurement, Minimum Mean Square Error Processed

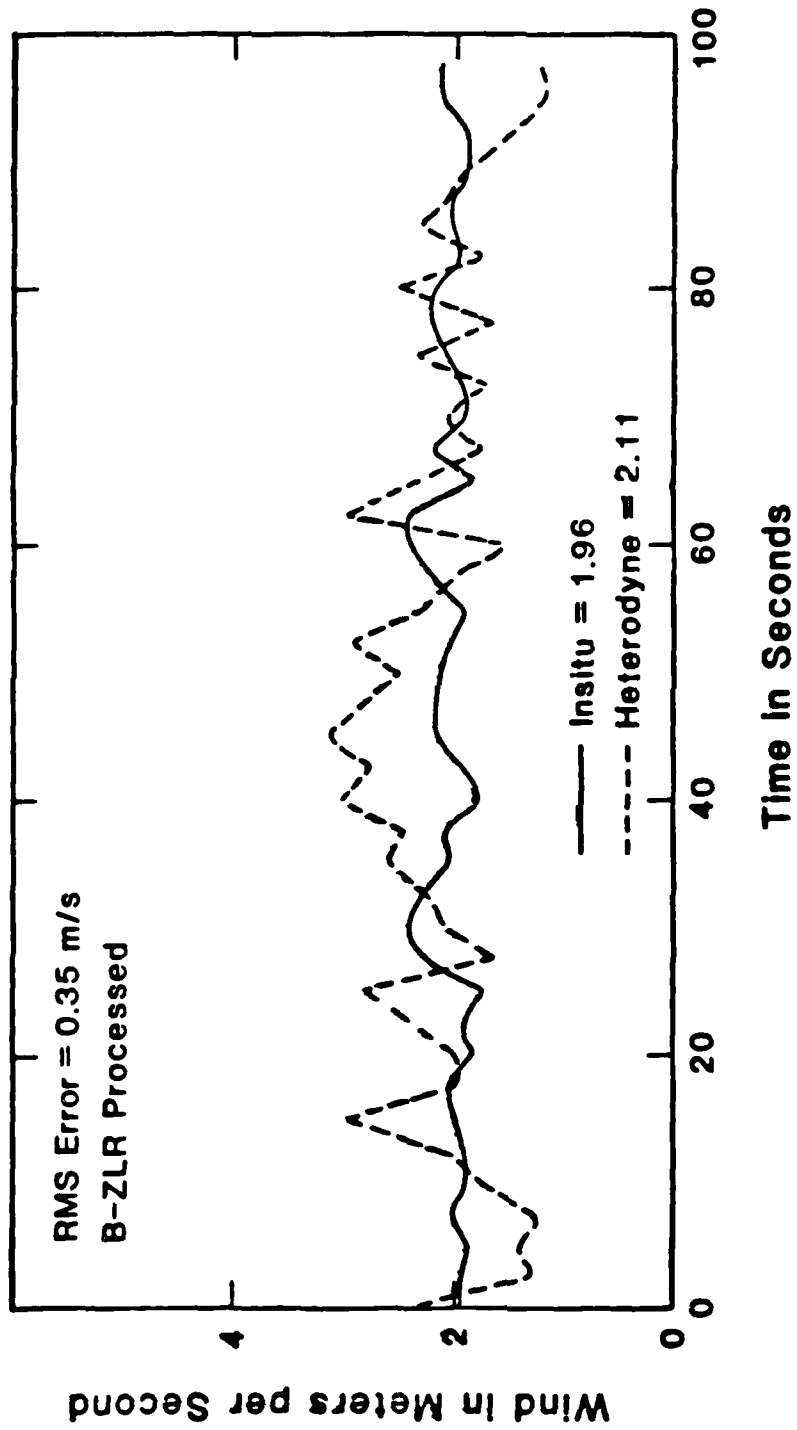


Figure 9 - Low Turbulence Wind Measurement, Binary-Z Log Ratio Processed

END

DATE

FILMED

4-88

DTIC